Arch. Mech., 42, 3, pp. 327–336, Warszawa 1990

The laminar boundary layer on a moving cylindrical rod

A. ZACHARA (WARSZAWA)

THE SUBJECT of this paper is a laminar boundary layer on a cylindrical rod moving in axial direction through a fluid at rest. Boundary layer equations have been reduced to one partial differential equation using the Mangler and Falkner–Skan transformations, with a nondimensional stream function as an unknown function. The equation was solved numerically. The results obtained have been presented in the form of integral boundary layer parameters as well as a skin friction coefficient and have been compared with the theoretical and experimental results obtained by other authors.

Przedmiotem pracy jest laminarna warstwa przyścienna na cylindrycznym pręcie poruszającym się w kierunku osiowym przez nieruchomy ośrodek ciekły. Równania warstwy przyściennej zostały przy użyciu transformacji Manglera i Falknera–Skana sprowadzone do jednego równania cząstkowego typu parabolicznego, zawierającego funkcję prądu jako niewiadomą. Równanie to zostało rozwiązane numerycznie. Otrzymane wyniki zostały przedstawione w formie całkowych parametrów warstwy przyściennej oraz współczynnika tarcia powierzchniowego i porównane z wynikami obliczeniowymi i eksperymentalnymi innych autorów.

Предметом работы является ламинарный пограничный слой на цилиндрическом стержне, движущимся в осевом направлении через неподвижную жидкую среду. Уравнения пограничного слоя, при использовании преобразований Манглера и Фолкнера–Скана, сведены к одному уравнению в частных производных параболического типа, содержавшему, как неизвестную, функцию тока. Это уравнение решено численным образом. Полученные результаты представлены в форме интегральных параметров пограничного слоя, а также коэффициента поверхностного трения и сравнены с расчетными и экспериментальными результатами других авторов.

1. Introduction

THE SUBJECT of this paper is a steady laminar flow induced by the motion of a cylindrical rod issuing from an orifice into a fluid at rest. Due to hydrodynamic friction, the fluid adjacent to the rod's surface is carried in the axial direction. At a short distance from the orifice, the flow takes the form of an axisymmetric boundary layer on the surface of the cylinder. The flow will be considered in frames of the laboratory reference system in which the velocity of the fluid on the rod's surface, equal to the velocity of the rod, decreases in normal direction to zero. The problem set here takes its origin in the field of man-made fibre spinning. The moving cylinder corresponds to the filament extruded from the spinneret and drawn in the axial direction through the fluid. The ambient fluid motion has a great influence on the process of fibre formation but not much attention has been paid to it in fluid dynamics research.

Papers on axisymmetric boundary layers are much less numerous than those on the boundary layers in plane geometry. The first meaningful works in this field of GLAUERT and LIGHTHILL [1] and STEWARTSON [2] are dated as late as the nineteen fifties and concern the flow past a stationary cylinder. SAKIADIS [3] was the first who calculated a flow

past a moving continuous cylindrical surface, making use of Pohlhausen's integral method with the Glauert–Lighthill logarithmic velocity profile. A similar approach has been applied recently by MAY [4] and KUBO [5] to a boundary layer on a filament with a velocity and diameter variable in the axial direction.

Apart from the Pohlhausen approach, methods of direct integration of boundary layer differential equations have also been used. CRANE [6] and KUIKEN [7] calculated a flow past a moving cylinder using series expansions and the obtained asymptotic solutions valid near the orifice ($x = 0$) and far down the cylinder ($x \to \infty$). The first numerical computations of axisymmetric boundary layer differential equations were made by JAFFE and OKAMURA [8]. Their computations, which concerned the case of a stationary cylinder, were carried out in the full range of x, without limitations involved in the papers [6] and [7].

The present paper, like the work [8], also contains numerical computations of axisymmetric boundary layer equations but these computations concern here a moving cylinder. The results obtained, presented in the form of integral boundary layer parameters, as well as a shear stress coefficient are compared with the results of SAKIADIS [3] and CRANE [6].

2. Governing equations and boundary conditions

We consider the steady, axisymmetric laminar boundary layer of an incompressible fluid on a continuous cylinder moving from an orifice in an axial direction at constant velocity through a fluid at rest. The radius of the cylinder and its velocity are denoted as a and U, respectively (Fig. 1). The flow is considered in frames of the boundary layer coordinate system in which the x-axis, parallel to the axis of symmetry, is posed along the solid surface and the y-axis is normal to it. The origin of the coordinate system is put in the plane of the orifice. The velocity components in the x- and y-directions are denoted by u and v, respectively.

We shall start with the general two-dimensional boundary layer equations [9]

$$\begin{cases} u\dfrac{\partial u}{\partial x}+v\dfrac{\partial u}{\partial y} = \dfrac{\nu}{r^k}\dfrac{\partial}{\partial y}\left(r^k\cdot\dfrac{\partial u}{\partial y}\right), \\ \dfrac{\partial}{\partial x}(r^k\cdot u)+\dfrac{\partial}{\partial y}(r^k\cdot v) = 0, \end{cases} \tag{2.1}$$

where $r(y) = a+y$.

These equations describe fluid flow in a plane as well as in axisymmetric geometry according to the value of the exponent

$$k = \begin{cases} 0, & \text{plane case,} \\ 1, & \text{axisymmetric case.} \end{cases} \tag{2.2}$$

The boundary conditions are as follows:

$$u(x,0) = U, \quad v(x,0) = 0, \quad \lim_{y\to\infty} u(x,y) = 0. \tag{2.3}$$

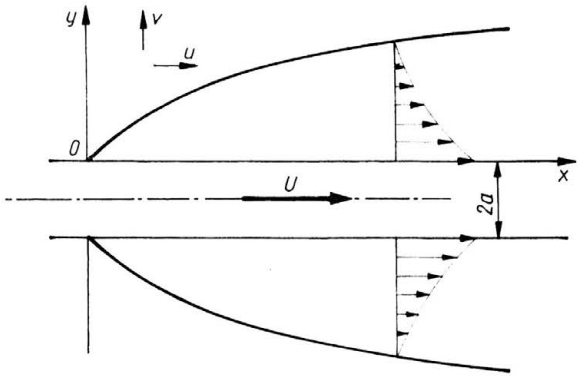

FIG. 1.

Now we shall put the system of Eqs. (2.1) into a nondimensional form using the combination of the Mangler and Falkner–Skan transformation [9]. To this aim we introduce the nondimensional normal coordinate η and nondimensional stream function $\bar{f}(x, \eta)$ defined as

$$\eta = \left(\frac{U}{\nu \cdot x}\right)^{1/2} \cdot y \cdot \left(1 + \frac{y}{2a}\right)^{k}, \tag{2.4}$$

$$\bar{f}(x, \eta) = \psi(x, y) \cdot (U\nu x)^{-1/2} \cdot a^{-k}. \tag{2.5}$$

The velocity components read then as follows

$$\begin{aligned} u &= \frac{1}{r^k} \frac{\partial \psi}{\partial y} = U \cdot \frac{\partial f}{\partial \eta}, \\ v &= -\frac{1}{r^k} \cdot \frac{\partial \psi}{\partial x} = -\left(\frac{a}{r}\right)^k \cdot \left(\frac{U\nu}{4x}\right)^{1/2} \cdot \left[\bar{f} + 2x \frac{\partial \bar{f}}{\partial x} - \eta \cdot \frac{\partial \bar{f}}{\partial \eta}\right]. \end{aligned} \tag{2.6}$$

Inserting the components (2.6) into Eq. (2.1), we obtain, after differentiation and some rearrangements, one partial differential equation (2.7) with $\bar{f}(x, \eta)$ as an unknown function:

$$\left\{\left[1 + \left(\frac{4\nu x}{Ua^2}\right)^{1/2} \cdot \eta\right]^k \cdot \bar{f}''\right\}' + \frac{1}{2} \bar{f} \cdot \bar{f}'' = x \cdot \left(\bar{f}' \cdot \frac{\partial \bar{f}'}{\partial x} - \bar{f}'' \frac{\partial \bar{f}}{\partial x}\right), \tag{2.7}$$

where the primes (′) denote differentiation with respect to η. This equation is valid for both plane and axisymmetric geometry. It is seen that its form for an axisymmetrical flow differs from that for a plane flow by the presence of the transverse-curvature term in square brackets. If a boundary layer thickness is much smaller than a body radius, this term may be neglected. However, in our case the boundary layer thickness may exceed many times the cylinder radius and the transverse-curvature term must be accounted for in Eq. (2.7). It is also worth noting that the boundary layer equation (2.7) in its axisymmetric version ($k = 1$) cannot be transformed to the self-similar form by taking x-derivatives equal to zero since the transverse curvature term will still be dependent on x.

We shall from now on limit ourselves to the axisymmetric version of Eq. (2.7). It is convenient to introduce a nondimensional variable in the axial direction

$$\xi = \left(\frac{4\nu x}{Ua^2}\right)^{1/2}, \tag{2.8}$$

and a new nondimensional stream function $f(\xi, \eta)$, which is equivalent to the stream function $\bar{f}(x, \eta)$ provided ξ and x satisfy Eq. (2.8). In these terms the velocity components u and v (2.6) can be expressed as follows

$$\begin{aligned} &\frac{u}{U} = f'(\xi, \eta), \\ &\frac{va}{\nu} = \frac{1}{\sqrt{1+\xi\cdot\eta}} \cdot \left[\frac{1}{\xi}(f'\cdot\eta - f) - \frac{\partial f}{\partial \xi}\right] \end{aligned} \tag{2.9}$$

and Eq. (2.7) takes its final form

$$[(1+\xi\cdot\eta)\cdot f'']' + \frac{1}{2} f\cdot f'' = \frac{1}{2}\xi\cdot\left(f'\cdot\frac{\partial f'}{\partial \xi} - f''\frac{\partial f}{\partial \xi}\right). \tag{2.10}$$

The boundary conditions (2.3) now read

$$f(\xi, 0) = 0, \quad f'(\xi, 0) = 1, \quad \lim_{\eta\to\infty} f'(\xi, \eta) = 0. \tag{2.11}$$

The governing equation (2.10) with ξ as an independent variable in axial direction is convenient in the region near the orifice ($\xi \ll 1$); however, far downstream ($\xi \gg 1$) it is advantageous to introduce a new ordinate [1]

$$\beta = \ln\left(\frac{4\nu x}{Ua^2}\right) = \ln(\xi^2). \tag{2.12}$$

The alternative form of Eq. (2.10) reads as follows

$$[(1+e^{\beta/2}\cdot\eta)\cdot f'']' + \frac{1}{2}\cdot f\cdot f'' = f'\frac{\partial f'}{\partial \beta} - f''\frac{\partial f}{\partial \beta} \tag{2.13}$$

with the boundary conditions the same as before Eqs. (2.11).

It should be noticed that Eq. (2.10) as well as Eq. (2.13) are given in a universal form and do not contain either the Reynolds number or any other free parameter.

3. Method of solution

Equation (2.10) is in fact a partial differential equation. However, if we replace derivatives with respect to ξ on the right hand side of this equation by suitable algebraic formulae, we may consider Eq. (2.10) as an ordinary differential equation with the η-coordinate as an independent variable. This approach was previously used by some authors for boundary layer calculations on a stationary body [8–11].

A fairly good approximation of the ξ-derivatives may be obtained with the use of the three-point backward difference relation derived from the Lagrange interpolation for-

mula for an unequally spaced mesh points. This approximation contains the new value f_n and two previously calculated f_{n-1} and f_{n-2}:

$$\left.\frac{\partial f}{\partial \xi}\right|_n \approx \frac{1}{\Delta\xi}\cdot[A_0(s)\cdot f_n + A_1(s)\cdot f_{n-1} + A_2(s)\cdot f_{n-2}],$$
$$\left.\frac{\partial f'}{\partial \xi}\right|_n \approx \frac{1}{\Delta\xi}\cdot[A_0(s)\cdot f'_n + A_1(s)\cdot f'_{n-1} + A_2(s)\cdot f'_{n-2}], \tag{3.1}$$

where

$$\Delta\xi = \xi_n - \xi_{n-1}, \quad s = \frac{\xi_{n-1}-\xi_{n-2}}{\Delta\xi},$$
$$A_0 = \frac{s+2}{s+1}, \quad A_1 = -\left(1+\frac{1}{s}\right), \quad A_2 = \frac{1}{(1+s)\cdot s}.$$

In the same way we shall approximate the derivatives $\partial f/\partial\beta$ and $\partial f'/\partial\beta$ from Eq. (2.13). Both forms of the governing equation are given below

$$[(1+\xi_n\cdot\eta)\cdot f''_n]' + \frac{1}{2} f_n\cdot f''_n = \frac{\xi_n}{2\cdot\Delta\xi}\cdot[f'_n\cdot(A_0\cdot f'_n + A_1\cdot f'_{n-1} + A_2\cdot f'_{n-2}) - f''_n\cdot(A_0\cdot f_n + A_1\cdot f_{n-1} + A_2\cdot f_{n-2})], \tag{3.2}$$

$$[(1+e^{\beta n/2}\cdot\eta)\cdot f''_n]' + \frac{1}{2} f_n\cdot f''_n = \frac{1}{\Delta\beta}[f'_n\cdot(A_0\cdot f'_n + A_1\cdot f'_{n-1} + A_2\cdot f'_{n-2}) - f''_n\cdot(A_0\cdot f_n + A_1\cdot f_{n-1} + A_2\cdot f_{n-2})]. \tag{3.3}$$

Equations (3.2) and (3.3) form an infinite set of ordinary differential equations, each of them corresponding to a given ordinate ξ_n or β_n. They are solved successively by a downstream-marching process starting from $n = 0$ ($\xi_0 = 0$) where Eq. (3.2) reduces to the Blasius equation. In the next mesh point $n = 1$ ($\xi = \xi_1$) the derivatives $\partial f'/\partial\xi$ and $\partial f/\partial\xi$ in Eq. (2.10) are approximated by two-point backward difference quotients. The form of Eq. (3.2) and (3.3) works for the mesh points $n \geqslant 2$ ($\xi_n \geqslant \xi_2$) downstream on.

Equation (3.2) was integrated in the ξ — direction at subsequent net points ξ_n until $\xi_n = 1$, which is equivalent to $\beta_n = 0$ (2.12). From this point Eq. (3.2) was replaced by Eq. (3.3) and the process continued until $\beta_n = 10$, which corresponds to $\xi \cong 148.4$. The process was stable and could be continued farther on.

The resulting ordinary differential equations were solved numerically by the Runge–Kutta–Gill algorithm adopted from [11]. While the boundary conditions at $\eta = 0$ could be directly introduced to the algorithm, the condition at infinity could be fulfilled by a shooting method in some approximation. A tentative value of $f''_n(0)$ was introduced and the equation was integrated up to the value η_1 at which the velocity profile $f'(\xi, \eta_1)$ had its minimum. The magnitude of this minimum was checked by the condition

$$f'(\xi, \eta_1) \leqslant \varepsilon. \tag{3.4}$$

If this condition was not satisfied, a corrected value of $f''_n(0)$ was put into calculations and the iteration continued. The Runge–Kutta algorithm was used with an increasing step size, starting from the value $h_0 = 0.025$. As a result of testing calculations, it was found that taking $\Delta\xi = 0.1$ and $\Delta\beta = 0.5$ leads to final results of good accuracy.

4. Results of calculations

Equations (3.2) and (3.3) were solved and velocity and shear stress profiles were obtained at each station ξ_n and β_n. In this section these results will be presented not in their detailed form but, for the sake of clarity, in the form of some commonly used boundary layer parameters, such as characteristic integral areae and shear stress coefficient. It will also make the comparison of our results with the results of other authors easier since they used the same type of presentation.

We shall first direct our attention to the integral parameters of a boundary layer, which are the displacement area Δ (4.1) and the momentum area Θ (4.2). In our notation they read

$$\frac{\Delta}{\pi a^2} = \frac{2}{U \cdot a^2} \cdot \int_a^\infty r \cdot u dr = \xi \cdot \lim_{\eta \to \infty} f(\xi, \eta), \tag{4.1}$$

$$\frac{\Theta}{\pi a^2} = \frac{2}{U^2 \cdot a^2} \cdot \int_a^\infty r \cdot u^2 dr = \xi \cdot \int_0^\infty f'^2(\xi, \eta) \cdot d\eta. \tag{4.2}$$

These parameters are presented as functions of the streamwise coordinates ξ and β in Figs. 2 and 3, respectively. The present results are compared here with those of SAKIADIS [3] and CRANE [6]. The Crane data presented in Fig. 2 are calculated from the formulae given in [6]

$$\begin{aligned} \frac{\Delta}{\pi a^2} &= \xi \cdot (1.62 + 1.16\xi) + O(\xi^3), \\ \frac{\Theta}{\pi a^2} &= \xi \cdot (0.888 + 0.190\xi) + O(\xi^3), \end{aligned} \tag{4.3}$$

derived on the basis of the asymptotic approximation valid for $\xi \ll 1$. A good agreement between the Crane results and ours is evident, even for ξ close to 1, which is outside the range of the adopted approximation. The same refers to the results in Fig. 3, where the data of Crane were calculated from the velocity profiles derived within frames of asymptotic approximation valid for $\xi \gg 1$ [6]. Here the Crane data start with $\beta = 4.29$ which corresponds to $\xi \approx 8.5$.

The results of SAKIADIS [3] obtained from an integral boundary layer equation cover the whole range of the streamwise coordinate ξ from 0 to infinity. They are also plotted in Figs. 2 and 3. The momentum area evaluated using of the Sakiadis method is in satisfactory agreement with the present results but his displacement area is highly underestimated in Fig. 2 as well as in Fig. 3. The discrepancy grows from about 30% near the orifice to over 60% at large axial distance. This rather surprising effect needs detailed examination. To this aim we shall compare the velocity profiles calculated by our method and by that of Sakiadis and deduce their influence on the integral boundary layer parameters.

Both profiles are plotted in Fig. 4, for the chosen axial coordinate $\beta = 4.29$. It is seen that while in the region close to the surface of the rod both profiles nearly coincide, in the

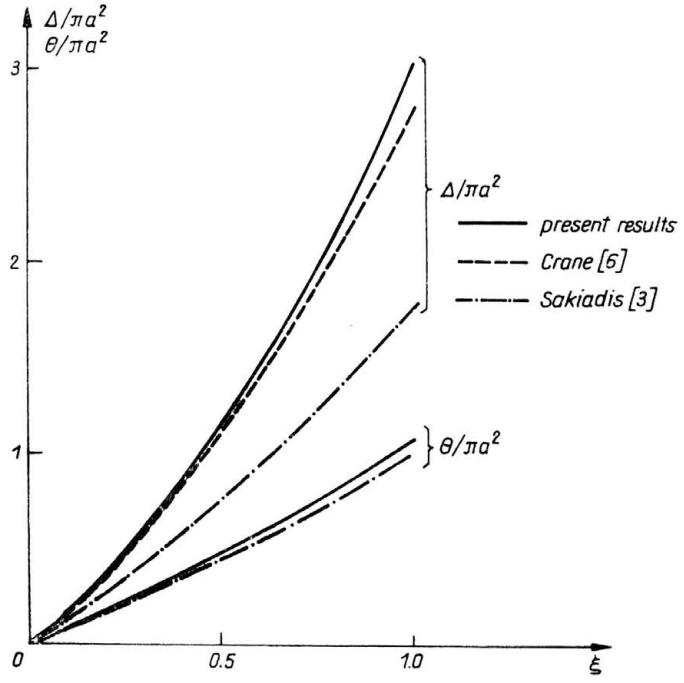

FIG. 2.

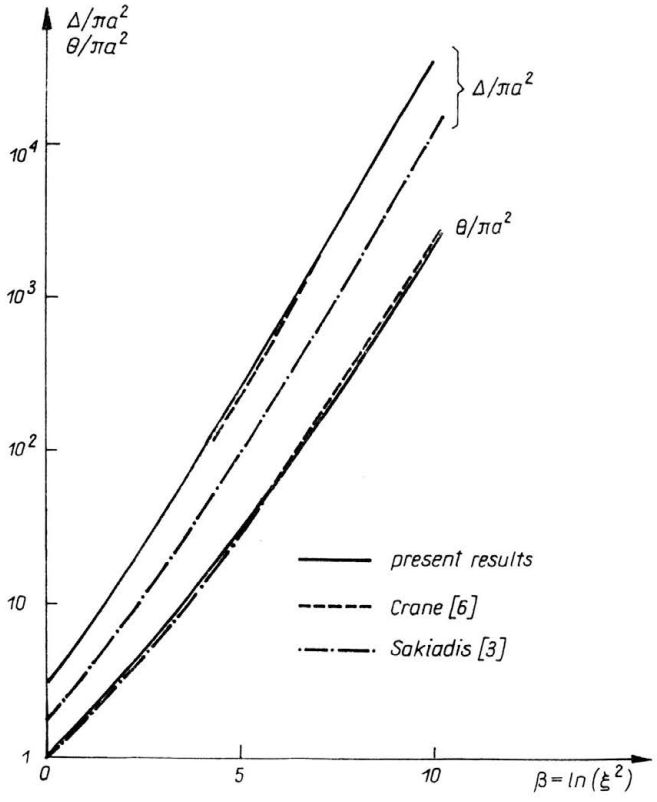

FIG. 3.

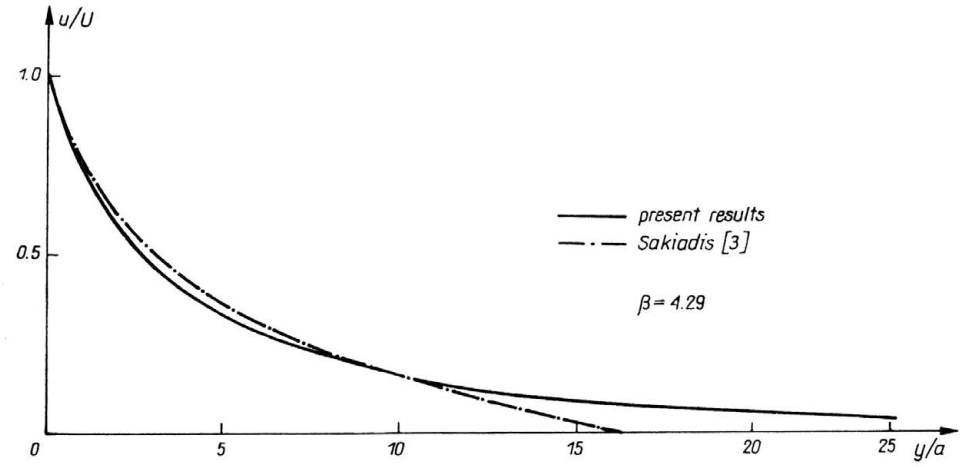

FIG. 4.

outer part the Sakiadis profile strongly deviates from ours. It does not fulfil the boundary condition at infinity, taking the value zero in finite distance from the surface. It is due to the logarithmic character of the adopted Glauert–Lighthill velocity profile.

The influence of the velocity profile on the integral boundary layer parameters Δ and Θ can be detected in Fig. 5 where the integrands from Eqs. (4.1)–(4.2) are presented.

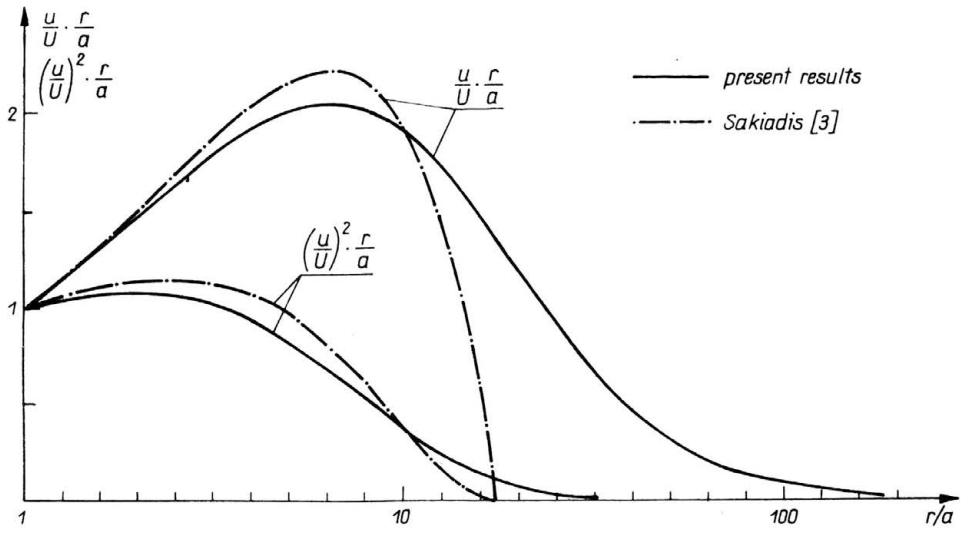

FIG. 5.

We can see that multiplication of the velocity profile by the normal ordinate, $(u/U) \cdot r/a$ makes the difference between our case and Sakiadis case even more pronounced. This explains why the displacement area in the Sakiadis case is so strongly underestimated. On the other hand, the square of the velocity profile in the integrand $(u/U)^2 \cdot r/a$ makes the difference between the two cases decrease, especially in the outer part of the layer

where $u/U \ll 1$. This is the reason for good agreement between our results and Sakiadis results in the case of the momentum area calculations.

We also calculated a wall friction coefficient which is defined as

$$c_f = \frac{-a \cdot \tau(x, a)}{\mu \cdot U} = -\frac{2}{\xi} \cdot f''(0), \tag{4.4}$$

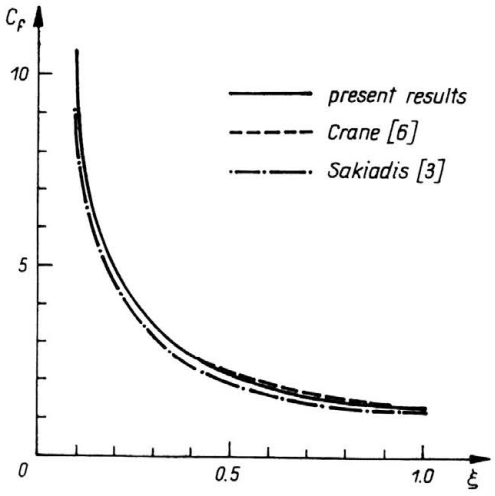

FIG. 6.

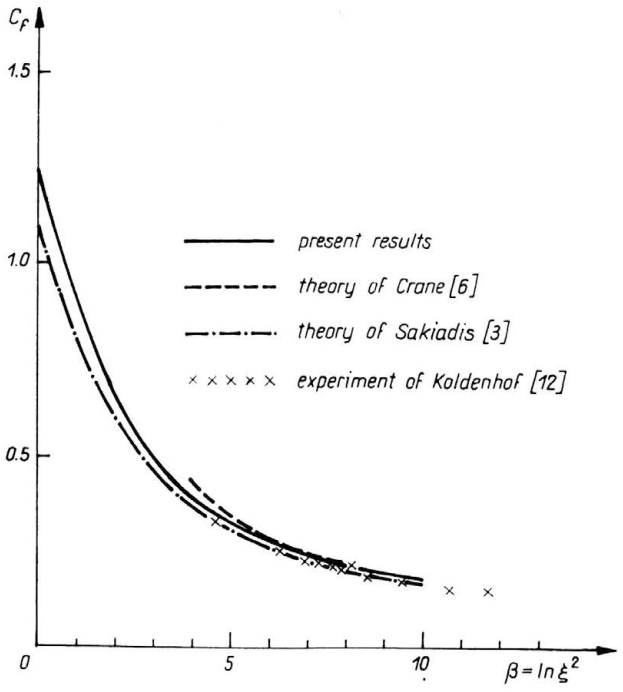

FIG. 7.

where $\tau(x, a)$ denotes shear stress at the rod surface. It has been plotted in Figs. 6 and 7 vs. the coordinates ξ and β, respectively, together with the corresponding results of SAKIADIS [3] and CRANE [6] as well as the experimental data of KOLDENHOFF [12]. It is seen that the agreement of all the results is very good. It indicates that all the methods compared here predict well the velocity profile near the surface of the cylinder.

The computational method presented in this paper appears to be a useful tool in calculations of axial boundary layers. It has helped to display the advantages and limitations of the existing approximate methods. We may expect that it will also work in more complex axisymmetric boundary layers involved in fibre manufacturing.

References

1. M. G. GLAUERT, M. J. LIGHTHILL, *The asymptotic boundary layer on a long thin cylinder*, Proc. Roy. Soc. (London), **A230**, 1181, 188–203, 1955.
2. K. STEWARTSON, *The asymptotic boundary layer on a circular cylinder*, Quart. Appl. Math., **13**, 113–122, 1955.
3. B. C. SAKIADIS, *The boundary layer on a continuous cylindrical surface*, AIChE. J., **7**, 3, 467–472, 1961.
4. S. MAY, *The thickness of the boundary layer on a stretching filament*, Arch. Mech., **36**, 2, 139–145, 1984.
5. S. KUBO, *Air boundary layer on a filament in high-speed spinning*, in: High-Speed Fiber Spinning, A. ZIABICKI and H. KAWAI [Eds.], Interscience, New York 1985.
6. L. J. CRANE, *Boundary layer flow on a cylinder moving in a fluid at rest*, ZAMP, **23**, 2, 201–212, 1972.
7. H. K. KUIKEN, *The cooling of a heat resistance cylinder moving through a fluid*, Proc. Roy. Soc. (London), **A346**, 1644, 23–35, 1975.
8. N. A. JAFFE, T. T. OKAMURA, *The transverse curvature effect on the incompressible laminar boundary layer for a longitudinal flow over a cylinder*, ZAMP, **19**, 4, 564–574, 1968.
9. T. CEBECI, P. BRADSHAW, *Momentum transfer in boundary layers*, Hemisphere Publ. Corp., Washington–London 1977.
10. A. M. O. SMITH, D. W. CLUTTER, *Solution of the incompressible laminar boundary layer equations*, AIAA J., **1**, 9, 2062–2071, 1963.
11. F. M. WHITE, *Viscous fluid flow*, McGraw-Hill Book, Comp., 1974.
12. E. A. KOLDENHOF, *Laminar boundary layers on continuous flat and cylindrical surfaces*, AIChE J., **9**, 411–418, 1963.

POLISH ACADEMY OF SCIENCES
INSTITUTE OF FUNDAMENTAL TECHNOLOGICAL RESEARCH.

Received November 20, 1989.